Icarus 225 (2013) 923–932

Contents lists available at SciVerse ScienceDirect

Icarus

journal homepage: www.elsevier.com/locate/icarus

Time scales of erosion and deposition recorded in the residual south polar cap of Mars

P.C. Thomas [a,*], W.M. Calvin [b], P. Gierasch [a], R. Haberle [c], P.B. James [d], S. Sholes [a]

[a] Center for Radiophysics and Space Research, Cornell University, Ithaca, NY 14853, USA
[b] Department of Geological Sciences, University of Nevada, Reno, NV 89577, USA
[c] Space Science Division, NASA Ames Research Center, Moffet Field, CA 94035, USA
[d] Space Science Institute, 4750 Walnut Street, Suite 205, Boulder, CO 80301, USA

ARTICLE INFO

Article history:
Available online 1 October 2012

Keywords:
Mars, Polar caps
Mars, Atmosphere
Mars, Climate
Mars

ABSTRACT

The residual south polar cap (RSPC) of Mars has been subject to competing processes during recent Mars years of high resolution image coverage: continuing erosion of scarps while the maximum extent grows as well as shrinks (Piqueux, S., Christensen, P.R. [2008]. J. Geophys. Res. (Planets) 113, 2006; James, P.B., Thomas, P.C., Malin, M.C. [2010]. Icarus 208, 82–85). Additionally, the cap has a variety of morphologies and erosion (scarp retreat) rates (Thomas, P.C., James, P.B., Calvin, W.M., Haberle, R., Malin, M.C. [2009]. Icarus 203, 352–375). Do these different forms and competing processes indicate an aging and possibly disappearing cap, a growing cap, or a fluctuating cap, and is it possible to infer the timescales of the processes acting on the RSPC? Here we use the latest imaging data from Mars' southern summer in Mars year 30 (Calendar year 2011) to evaluate erosion rates of forms in the RSPC over 6 Mars years, and to map more fully features whose sizes can be used to predict deposit ages. Data through Mars year 30 show that scarp retreat rates in the RSPC have remained approximately the same for at least 6 Mars years and that these rates of erosion also apply approximately over the past 21 Mars years. The thicker units appear to have undergone changes in the locations of new pit formation about 30–50 Mars years ago. The thinner units have some areas that are possibly 80 Mars years old, with some younger materials having accumulated more than a meter in thickness since Mars year 9. Formation of the thicker units probably required over 100 Mars years. The upper surfaces of most areas, especially the thicker units, show little change at the few-cm level over the last 2 Mars years. This observation suggests that current conditions are substantially different from those when the thicker units were deposited. A prime characteristic of the evolution of the RSPC is that some changes are progressive, such as those involving scarp retreat, while others, such as the geography of initiation of new pits or the areal coverage of ice, appear to be more episodic.

1. Motivation

CO_2 follows an annual cycle of deposition and sublimation on the poles of Mars. At present there is no CO_2 deposit that survives the northern summer, while there is an area of >80,000 km^2 near the south pole that has a perennial CO_2 surface deposit. This perennial deposit has been visible for more than 100 Earth years thus is the net result of climate over more than 50 Mars years. The total amounts and different depositional units in the RSPC record a history of the CO_2 mass balance. As with discussions of terrestrial climate variations, the timescales of variability on Mars carry different implications for their causes and for their geological significance. While the RSPC has been observed by spacecraft for over 20 Mars years, and has been visible to Earth-based observers for more than a century, it may contain information on longer time scales as well.

The finding that some of the RSPC was undergoing year-to-year erosion (Malin et al., 2001) suggested that the RSPC might have a limited lifetime and that its loss represents a change in climate from that responsible for its deposition. The observed rates of erosion and the size of the eroding pits suggested that the RSPC had been in existence for over a Mars century (Byrne and Ingersoll, 2003a; Thomas et al., 2005). Further high resolution studies over the most recent few Mars years (MY 24–29) showed that erosion of pits and scarps continued, but that the area covered by the RSPC fluctuated by a few per cent (Thomas et al., 2009; James et al., 2010). Studies of the first 18 Mars years of spacecraft data showed that the extent and patchiness of the residual cap varied slightly year-to-year (Piqueux and Christensen, 2008), but the overall late summer coverage appears quite similar over 21 Mars years.

* Corresponding author.
E-mail address: pct2@cornell.edu (P.C. Thomas).

0019-1035/$ - see front matter © 2012 Elsevier Inc. All rights reserved.
http://dx.doi.org/10.1016/j.icarus.2012.08.038

Modeling of sublimation and deposition has suggested that pitted landscapes might erode in cycles controlled by surface roughness effects and unusual annual deposition that might mimic appearances of an evolving cap (Byrne, 2011). Haberle and Kahre (2010), Kahre and Haberle (2010) and Haberle et al. (2009) conclude that surface pressure measurements may indicate a changing Mars atmospheric mass that is consistent with progressive loss of material from the RSPC after MY 12 when the first surface pressure measurements were made by Viking landers.

The purpose of this investigation is to use image data obtained through MY 30 to evaluate possible time spans represented by different physical units in the RSPC. The variety of model and observation results noted above show a need to clarify the lengths of any periods of possible climate variability recorded in the cap. We first review the measurement results on rates of change in the RSPC and the different morphologic units. We then present new measurements of rates of change in the different morphologic units. From these data we infer the different times when deposits were eroding and when they may have initially formed. Finally we note some of the other constraints on modeling the history of the RSPC.

2. Data, types of observations, definitions

We use images from Mars Observer Camera (MOC) with pixel scales of 1.5–2.4 m (Malin et al., 1992), Mars Reconnaissance Orbiter's Context Imager (CTX, Malin et al., 2007) and High Resolution Imager and Science Experiment (HiRISE, McEwen et al., 2007), and Mariner 9 images (Levinthal et al., 1973). The Mariner 9, MOC and CTX images have been map projected to appropriate scales for either mapping or for comparison with HiRISE using software developed at Malin Space Science Systems. The HiRISE data are standard map projected products with 25- or 50-cm pixels. The basis for mapping of morphologic units in the RSPC is a 6 m/pixel mosaic of southern summer images, Mars Year (MY) 30 (2011). Digitizing measurements of locations and sizes of features are all referenced to this polar stereographic projection. Uncertainties in mapped positions can be well over 100 m, but our primary concern here is relative measurements over short distances. These can be controlled to under 1% variation by rescaling overlaid images of the same areas obtained at different times. Year-to-year change measurements of MOC and HiRISE data are done on Photoshop® layered versions at the same scale such that measurements at different years accurately cross the same path. In the year-to-year measurements the L_s of both images are used to scale the part of each season's change for an accurate baseline of the applicable time span. Within-year changes reported in James et al. (2010) provide the basis for this scaling. Change measurements reported here span either 5 or 6 Mars years; the fractional changes in diameters resulting from use of time spans rounded to integer year values would be generally less than 10% (half of 1 year's change divided by 5 or 6 Mars years).

The different images, MOC and HiRISE, have similar map projections but referenced to different topographic models. These different reference surfaces impart small differences between maps, but the local scales are constrained to well within 1% on all images of one area by scaling the overlaid images; usually this involved only a few pixels out of several thousand. The diameters, or distances across depressions, are measured manually, scarp-to-scarp, on those pits where sharp boundaries are visible on diametrically facing scarps. Diameters so measured are probably good to no worse than 2 pixels. Changes over 6 Mars years are in the 25–50 m range, so errors of even 2 pixels (3 m) are mostly no more than 10% of the value. Because the scarps change during each summer, are never completely straight, and involve tilting and seasonal sublimation, little would be gained by doing photometric edge detection.

The Mars years are referenced to the calendar developed by Clancy et al. (2000), which has Mars year 1 beginning at solar longitude of 0 on April 11 1955. We use "MY" to mean a calendrical Mars year, and the symbol "♂y" to designate periods of time in Mars years. In descriptions of the features in the residual cap

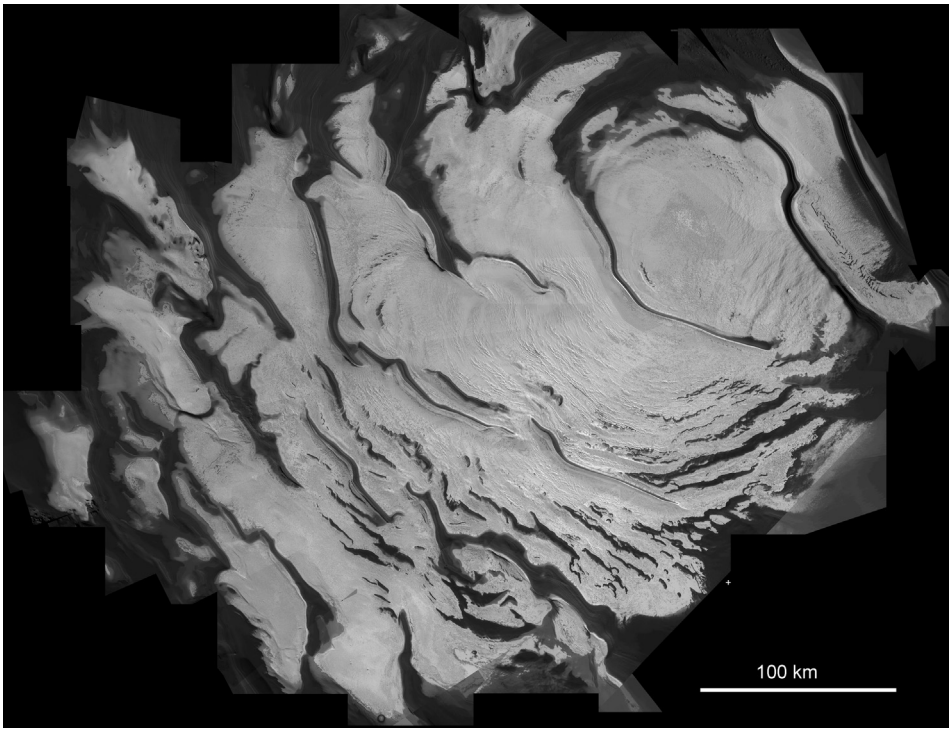

Fig. 1. Residual south polar cap MY 30. CTX image mosaic; data obtained between L_s 327° and L_s 346°. Small cross above left of scale bar is south pole; 0 longitude is toward top.

Table 1
Unit characteristics.

A0	~8–14 m in thickness, average probably ~10 m. Occurs in largely elongate outcrops scattered over the RSPC, usually near edges of large troughs. Upper surface shows polygonal trough patterns. Depressions within this unit are large, nearly circular, up to 1400 m in diameter. Total area ~270 km^2
A1	~8 m in thickness, occurs primarily in a region centered at ~87S, 10W. Upper surface has polygonal troughs, usually more distinct than those of unit A0. Depressions are largely asymmetric ("curled" in shape), and unimodal in size around a mean diameter of ~200 m (MY30). Total area ~1200 km^2
A2	~6–8 m thick, distinguished by linear troughs with asymmetric profiles. These troughs in some regions grade into curled depressions typical of unit A1. Total area ~8000 km^2
B	~0–3 m in thickness, covers most of the RSPC. Varied density, size, and shape of depressions. Upper surface smoother than that of A0 and A1. Total area ~77,000 km^2

"pit" is used to designate nearly round depressions; most are very shallow compared to their diameters.

3. Morphologic units of the RSPC

The surface of the RSPC (Fig. 1) can be divided into a few morphologic units based on surface texture, pit sizes, apparent thickness, and stratigraphic relations (Thomas et al., 2009). Here we summarize only the broad characteristics of the units applicable to this work (Table 1).

The oldest and thickest unit is A0, characterized by an upper surface with polygonal troughs and ridges, thickness of 9–14 m (averaging slightly more than 10 m, determined from Mars Orbiter Laser Altimeter (MOLA) and shadow data), and pits of 100–1000 m in diameter (Fig. 2a and d). Unit A1 has an upper surface somewhat similar to that of A0, but is thinner, ~8 m, occurs in larger contiguous areas, and has smaller, usually asymmetric, depressions (Fig. 2b and e). A2 is the so-called "fingerprint" terrain as it is characterized by linear and tuning-fork shaped depressions, and in places grades into unit A1. Unit B covers most of the RSPC and is probably everywhere less than 3 m in thickness (Fig. 2c and f). Its upper surface is smoother in HiRISE and MOC images than are the A units (Compare Fig. 2d–f), although there are some ridges and cracks visible in HiRISE data. It overlies A units, including interiors of unit A0 pits, and some of this unit was observed to form after MY 9. The shape and sizes of pits in Unit B vary greatly, indicating the possibility of a range of deposit physical properties and exposure and erosional histories.

4. Rates of erosion in the RSPC

Previous comparisons of changes within the RSPC using MOC images indicated that the different units undergo erosion by scarp retreat at different rates. The rates we derive are the meters per Mars year that a scarp crest retreats. Usually these are measured across depressions or mesas such that total changes are twice the single-face retreat rate. In a few instances (<5) we have measured single face retreat by reference to positions of crossing troughs that do not change year-to-year. Here our data are from MY 24 or 25 for MOC data at 1.5 m/pixel, and MY 30 data from HiRISE at 25 or 50 cm/pixel. Comparison measures are made at 1.5 m pixel projections. There are limited areas with repeat MOC and HiRISE coverage, so the number of measurements is small. Thomas et al. (2005) reported a variety of measures of A unit scarp retreat rates at 3.3–3.8 m/♂y, and unit B rates at 2.3 ± 0.5 m/♂y. Updated data in Thomas et al. (2009) gave unit A0 rates of 3.8 ± 1.1 m/♂y, A1 as 3.3 ± 0.6 m/♂y, and B as 2.2 ± 0.7 m/♂y. Table 2 gives our newer results. These are very close to previous values and emphasize the findings of James et al. (2010) that the scarp retreat rates continue at roughly the same level despite changes in year-to-year residual cap extent.

We emphasize earlier results that showed the erosion of the scarps is not a simple retreat of a sublimating face (Byrne et al., 2008; Thomas et al., 2009). There is a complicated series of steps shown by HiRISE data (and MOC) of fracturing near the scarp crest,

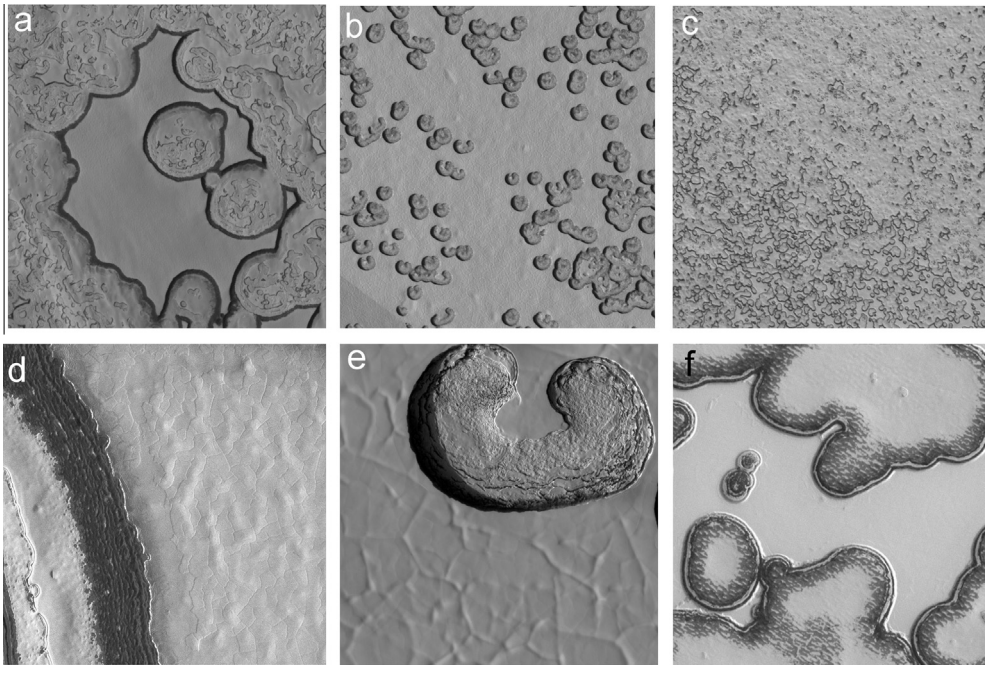

Fig. 2. Selected units of the RSPC. Top panels all 4.5 km in width. Bottom panels all 0.3 km in width. Sun is from left in all panels. (a) Mesa of unit A0 materials with bounding darker debris apron, CTX MY 30. (b) Unit A1. CTX. (c) Unit B, CTX. (d) Unit A0, HiRISE, image ESP_023779-0930. (e) Unit A1, HiRISE ESP_023638-0930. (f) Unit B, HiRISE ESP_023680-0930.

Table 2
Scarp retreat rates.

Unit and time	Data	m/$\Im$y s.d.	No.
A0 MY 27[a]/28–30	HiRISE/HiRISE	4.4 ± 0.6	19
A0 MY 24–30	MOC/HiRISE	4.4 ± 0.7	20
A1 MY 24–30	MOC/HiRISE	3.6 ± 0.2	19
B MY 24–30	MOC/HiRISE	2.4 ± 0.5	50

[a] Some data taken in spring of MY28 effectively show state at end of MY27 summer.

block failure and rotation, and subsequent gradual loss of material for several Mars years. This eventual loss of material is undoubtedly by sublimation. For the thick A0 materials, debris left by the passage of a retreating scarp can take over 15 Mars years to completely disappear. For some materials in the RSPC subsurface pressurization might play a role in erosion (Pathare et al., 2005). Local cycling of volatiles occurs near scarps in the RSPC (Becerra et al., 2011) but it is not clear that this process has significant effects on scarp retreat mechanisms or rates.

It is also important to note that the stratigraphy within individual units is unclear due to the lack of exposed layering. Some crudely parallel markings near scarps were interpreted from MOC data to be layer outcrops (Thomas et al., 2005). HiRISE data, however, clearly show these forms to be debris left by the retreat of scarps and not exposed layers (Thomas et al., 2009). There are some layers $\ll$1 m thick exposed on the upper surfaces that may help in interpreting the deposition of materials. These layers are discussed in Section 7 below.

5. Unit ages and observable timescales

We attempt to delineate periods of erosion and deposition in the RSPC by using sizes of expanding depressions and their scarp retreat rates in combination with observations of the minimum/maximum age of certain units.

Previous work extrapolating current scarp erosion rates back to Mariner 9 observations in Mars year 9 gave predictions of ages of some features in probable post-Mariner 9 materials close to Mars year 9 (Thomas et al., 2005). Here we expand those results relying on: (1) The updated and more accurate erosion rates calculated from the newer data (MY 30) and (2) the complete and essentially uniform imaging of the summer cap in 2 Mars years at 6 m/pixel which allows a complete survey of forms within the residual cap.

The A0 and A1 units stand as designated in Thomas et al. (2009). The thinner B unit, comprising the vast majority of the cap, has a variety of depressions previously measured in great detail (Thomas et al., 2005, 2009) and a range of thicknesses and surface textures.

5.1. Pre- and post-mariner 9 smooth materials

Two parts of the B units can be segregated on the basis of Mariner 9 data obtained in MY 9. These are shown at two spatial resolutions in Figs. 3 and 4. Some relatively bright, distinctively shaped areas of the RSPC seen in Mariner 9 data survive until MY 30 (Fig. 3). Mariner 9 images better than 100 m/pixel covered only parts of the residual cap; in these limited areas we are able to map these B unit materials existing at Mars year 9, and areas that were deposited sometime after MY 9. These selected areas are mapped in Fig. 5a. Viking data showed substantial brightening of many areas after Mariner 9 (Fig. 3; James et al., 1992; Piqueux and Christensen, 2008). The sequence shown in Fig. 3. demonstrates that development of these deposits was progressive after Mariner 9 and not a single change that occurred between Mars years 9 and 12. HiRISE views (Fig. 4c) show that these deposits have measureable thicknesses in some places (discussed in more detail in Thomas et al., 2009). Shadows in pits in the unit shown in Fig. 4c indicate a depth of just over a meter. These post-Mariner 9 deposits are especially useful in testing the applicability of pit erosion rates as the age of the whole deposit is definitively limited. We note that the areas selected for measurement are only a part of the pre- and post-Mariner 9 visible deposits, but their clear identification as fitting one category or the other allows good tests of what has occurred in such deposits. An illustration of the widespread nature of changes that occurred after Mariner 9 is the presence of "worms." These are sinuous troughs marking contacts of areas with post-Mariner deposits with thicker, older materials, nearly all of these being different parts of unit B. Measurement locations are mapped in Fig. 5b.

5.2. Pit sizes in the various deposits

Fig. 6 summarizes the measured pit sizes. The depressions in unit A0 are the largest and most circular of the pits in any RSPC

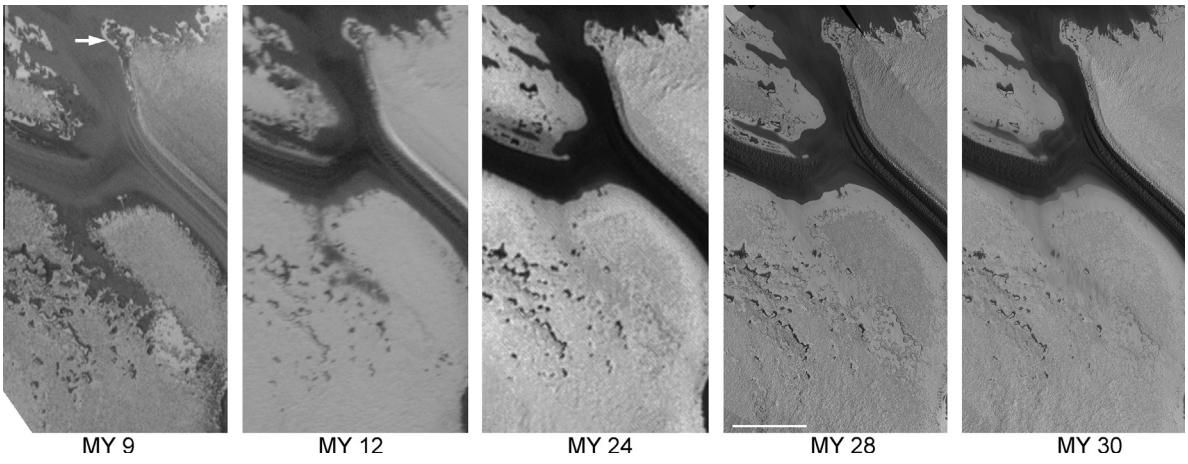

Fig. 3. RSPC changes from Mariner 9 to MRO. From left: MY 9: Mariner 9 image 231b01; L_s = 356°; MY 12: Viking Orbiter image 421B77, L_s = 348°; MY 24: MOC WAC image, M15-01108, L_s = 345°; MY 28: CTX images mostly P13_06176_0935_XN_86S350W (L_s = 350.4°); and P13_05951_0928_XI_87S341W (L_s = 341°); MY 30: CTX images parts of G13_023410_0945_XI_85S003W, G13_023384_0944_XI_85S014W, G13_023463_0944_XI_85S011W, G13_023291_0943_XI_85S354W, L_s = 329° to L_s = 336°. Scale bar is 10 km. These images have been separately contrast enhanced. Solar incidence angles vary slightly, but distribution of high contrasts is the important element in these comparisons. Low albedo coverage is progressively less in time in the left three panels; there is much less change among the last three panels but change is still progressive. Note preservation of relatively small dark areas in lower left, and preservation of many boundaries even though the overall contrasts vary. Center of panels is 86°S, 358°W.

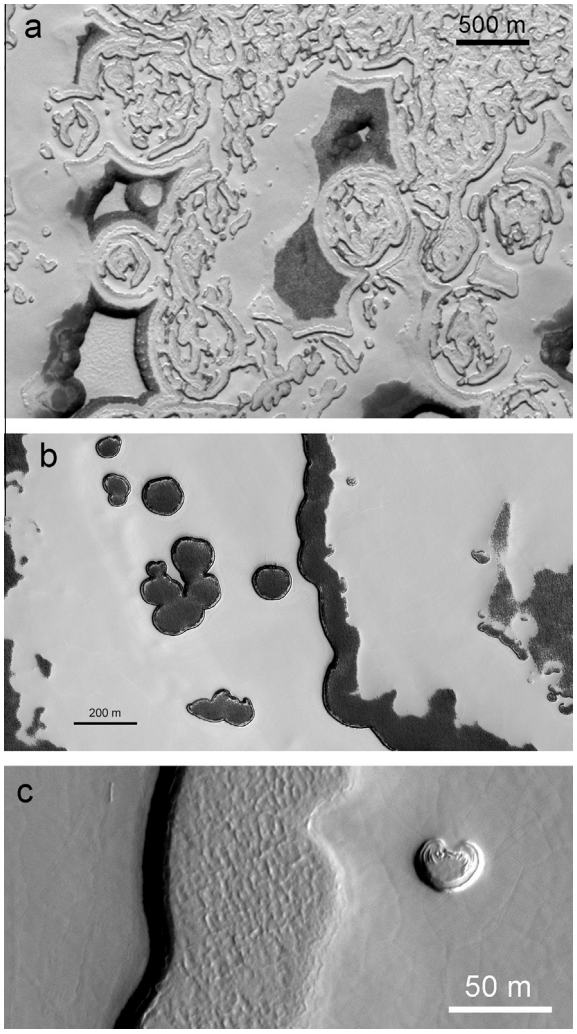

Fig. 4. Examples of variation in depressions and in depositional units: ghost depressions and two ages of unit B. (A) "Ghost" depressions of unit A0. Only small remnants of the actual A0 are left, but nearly circular patterns eroded in unit B that had filled older depressions in unit A0 are clear. Portion of CTX image G14_023542_0937_XI_86S_000 W, L_s = 339.5°, center at 86.4°S, 357.6°W. (B) Pre- (left side of dark, sinuous area) and post-Mariner 9 deposits (right side); see arrow in Fig. 3 for location. Much of this later material was deposited after the Viking observations in MY 12. Note the larger, more numerous pits in the older materials. Darker area separating these materials is one of the "worms." HiRISE image ESP_023792-0940, L_s = 349.7°, center at 85.8S, 357.3°W, MY 30. Strongly contrast enhanced. (C) Close view of two parts of unit B, upper middle part of panel (B) with shadows from scarps in both units. HiRISE image ESP_020720_0940, L_s = 206.5°, i = 79.5°, 85.77S, 357.54°W.

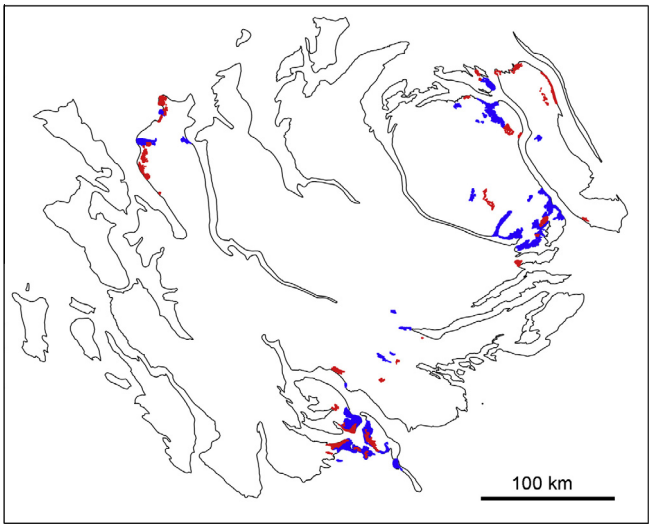

Fig. 5a. Selected areas of pre-Mariner 9 smooth materials (red), and post-Mariner 9 materials (blue) used for pit size measurements. Outlines show approximate RSPC extent in MY 30.

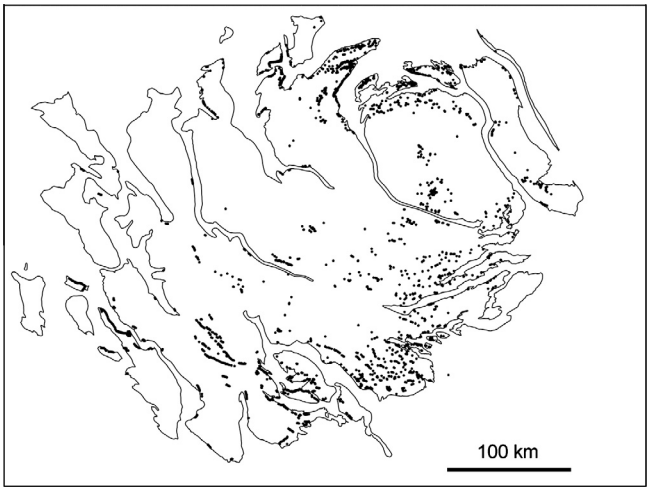

Fig. 5b. Locations of "worms" mapped in MY 30 CTX mosaic. These forms indicate boundaries of pre- and post-Mariner 9 smooth deposits.

unit. A few are over a km across, and there is a broad distribution of sizes between 400 and 1000 m. A secondary population is 200 m or less in diameter. Remnants of other large A0 depressions, termed "ghosts" (Fig. 4a), illustrate some complexity in the combined histories of units A0 and B. These "ghosts" are largely free from A0 remnants and are marked by semi- or fully circularly-symmetric patterns eroded in unit B identical to those erosional patterns of unit B within fully enclosed pits in unit A0. The "ghost" forms of these depressions, numbering only 40 (vs 498 for the A0) are nearly all between 300 and 800 m across.

The heart- or bean-shaped depressions in A1 have been measured at the maximum symmetric widths (roughly horizontally in Fig. 2e), and we have not included those with large central mounds or ramps, because these forms grade into very elongated ones of the "fingerprint" terrain, and the distance between opposite sides would be much larger than the distance traversed by a retreating scarp. These diameters are strongly peaked at slightly more than 200 m, with a small increase under 50 m width. These results are close to those obtained from a more restricted sampling area reported in Byrne and Ingersoll (2003a).

Pits formed in the portions of unit B identified as smooth, pre-Mariner 9 materials have different size distributions from those in materials deposited after MY 9, as expected. The pre-Mariner 9 surfaces have a broader peak in the size distribution of pits, centered at larger sizes, and have a small population of pits up to 500 m across. Pits in the materials deposited after MY 9 have diameters up to slightly over 100 m with an average size of 68 ± 30 m (s.d.). The difference in pit sizes and frequency in these two units is apparent in Fig. 4b.

Pits in other parts of unit B, reported in Thomas et al. (2009) and shown in Fig. 6d also have a tail extending to diameters of 400 m. We note that the full size distribution is strongly affected by selection effects and Fig 6d is not a snapshot of a complete unit B pit size distribution. It does show that some areas of unit B, have existed long enough to accumulate some pits far larger than the average size of unit B pits.

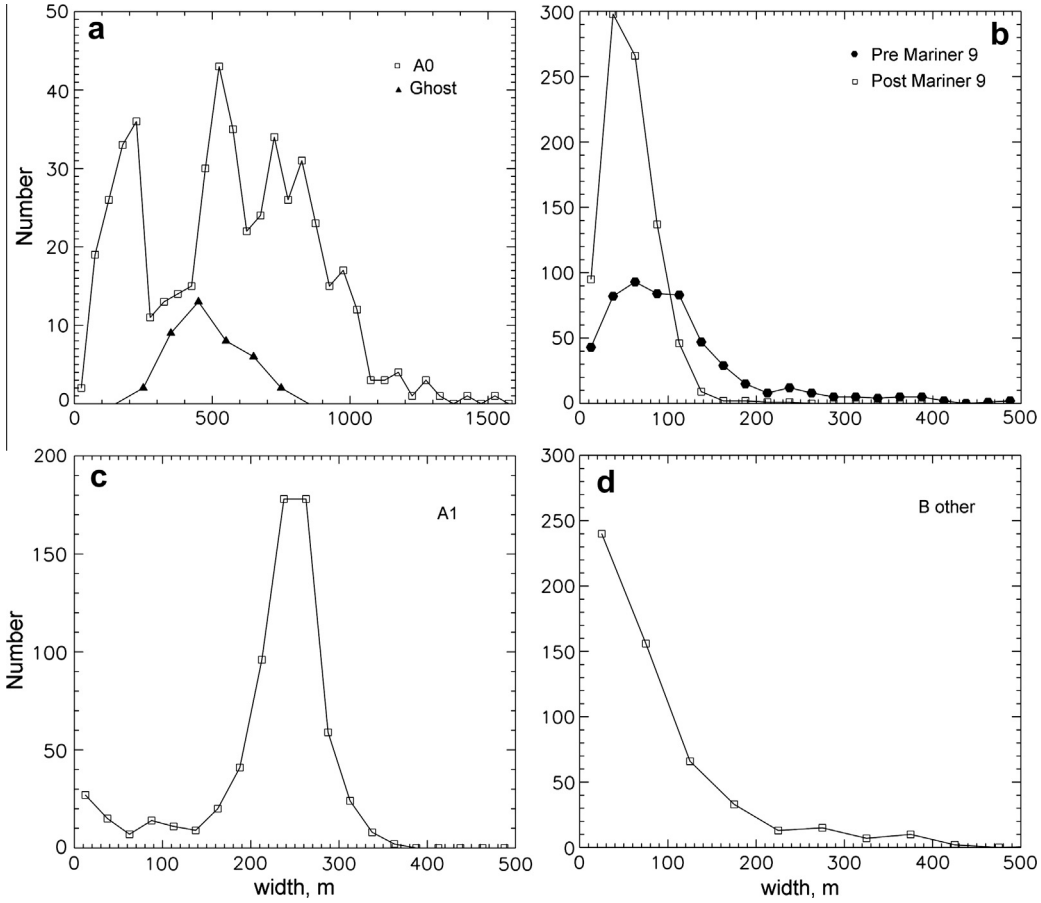

Fig. 6. Pit size distributions in selected RSPC units. Note that the pits sampled in (d) are from several widely scattered areas of the RSPC and do not include areas in (b), and should not be taken as a complete size distribution for a particular deposit.

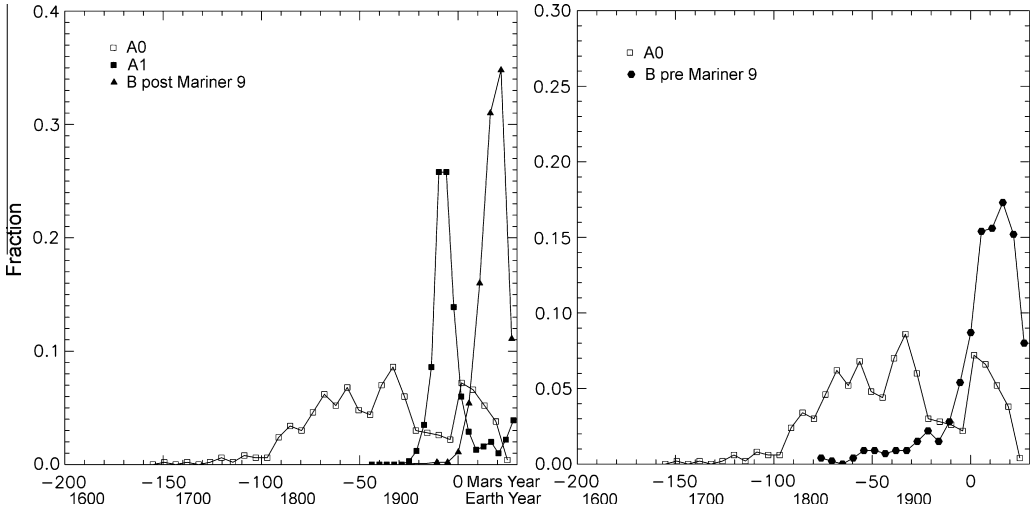

Fig. 7. Mars years of activity of erosion of pits in different units assuming constant scarp retreat rates applied to pit sizes plotted in Fig. 6. Ages are simply the full widths divided by 2, divided by the appropriate retreat rate. Years are the ages subtracted from Mars year of observation.

6. Modeled ages and timescales

6.1. Evaluating distribution of pit sizes with expansion rates

Combining the observed pit size distributions with average scarp retreat rates involves uncertainties in the rates measured over a few Mars years, questions of the applicability of these rates to longer periods, and possible spatial variations in erosion rates within otherwise similar units. Uncertainties in the measured rates, 6–21% (Table 2) are small compared to the spread of the size distribution peaks of A0 (larger group) and pre-Mariner 9 unit B shown in Fig. 6b. Even for the A1 depressions, the standard deviation of the primary peak in diameter distribution, 15% of the mean value, is large compared to that of the rate measurements (6%).

Because the spread of current rate measurements is smaller than that of the pit widths, a first approximation assumes the range of widths is a range of ages. For this approach we have plotted the model ages for the different units in Fig. 7, using our size measurements and accounting for which Mars year they were obtained.

Unit A0 appears to have had a period of erosion, nominally 80 ♂y of pit initiation, followed by a reduced period of pit formation, in turn followed by the last ~30 ♂y of erosion. This unit was in existence approximately at −100 MY if current rates of erosion applied and there were no interruptions in that erosion. The time scales in this work differ by 5–20% from those of Thomas et al. (2009) due to the improved and slightly greater erosion rates calculated for A0.

The peak formation time of the pits in post-Mariner 9 smooth units extrapolates to MY 9. This result provides some further confidence in extrapolating back more than the current 6 ♂y of high resolution observations. A few pits have diameters that would predict ages slightly older than MY 9; as the deposit is well constrained in maximum age, these give some indication of the variability of combined effects of rates, merging pit forms, initial pit sizes, or other unaccounted processes. These are less than 10% of the sample, and if anything provide some reassurance that the real age "signal" in these sizes and rates is good.

Pits in unit A1, with their sharply peaked size distribution, extrapolate to a formation period of ~MY −10, which with the assumptions being used, falls within the period of low rate of initiation of new pits in unit A0. Byrne and Ingersoll (2003a) also found a restricted size distribution and concluded initiation of pit erosion occurred over a small time interval.

The pits in the selected pre-Mariner 9 smooth areas extrapolate to as early as MY ~−60; other unit B pits measured would reach about the same age (Fig. 6d). The large range of B unit inferred ages and the range of morphologies are all part of the range of patchiness observed by Piqueux and Christensen (2008).

We note that the considerable area of the RSPC displaying fingerprint terrain (Thomas et al., 2005, 2009) is not included in our rate survey. These forms in cross section are sharp retreating scarps facing smooth, gentle crests. The latter are extremely difficult to compare year-to-year due to the scarcity of nearby markings on an upper surface that survive as fiducial marks. There is some evidence these forms involve both widening of the troughs as well as some advance of the smooth slopes, but detailed investigations of these forms are beyond the scope of this work.

6.2. Extrapolating current rates backwards

The erosion rates of scarps in the RSPC appear to be stable over the last 6 Mars years. This period includes some significant variations in the annual dust loading and in the possible thermal balances (Bonev et al., 2002; James et al., 2010). The sizes of pits within the post-Mariner 9 deposits are consistent with expansion rates being stable for 20 ♂y in these parts of Unit B. The more widespread measurements (Fig. 5b) of the "worms" which mark edges of post-Mariner 9 (and some post-Viking) deposits and extrapolate with B-unit rates back to MY 10 (±4 ♂y) also suggest that average recent conditions have applied over this interval.

Direct comparison of forms in Mariner 9 images to more recent data is now possible for the more rapidly-changing forms. Observations in Mariner 9 images of the RSPC used here are at 94–112 m/pixel. Comparisons of MY 9 and MY 30 data are done with map projected images at uniform pixel scales, but depend upon use of topographic models and thus may include some different distortions in the projections of data from different spacecraft. Our expected diameter change at single-face retreat rates of 4.4 m/♂y for unit A0 over 21 Mars years is 92 m, or just under one raw Mariner 9 pixel. Given good contrasts we might expect to statistically see differences in widths of septa or in diameters of pits (~180 m of predicted changes). Comparisons are limited because most A0 outcrops are only a few pixels across in Mariner data. These small features make consistent selection of lines in both sets of data difficult. However, we have made 25 measurements of A0 features that yield an average retreat rate between MY 9 and MY 30 of 3.5 ± 1.8 m/♂y, with values ranging from 0.4 to 8.7 m/♂y. Thus, scarp erosion in the last 21 Mars years appears to be consistent with that measured in detail over the last 6 Mars years.

Features noted in Thomas et al. (2005) suggest that there have been instances of changed conditions between MY 9 and MY 24. These forms include the "moats:" depressions flanking mesas of units A and B, often forming within depressions in these depositional units and distinct in size and appearance from the "worms." The bi-modal distribution of moat widths suggests specific depositional events approximately at Mars years 10 and 20 (Thomas et al., 2005). The more recent and smaller moats are nearly invisible in HiRISE data from MY 30. This loss of visibility may could be due either to erosion blurring these very low (<1 m?) scarps, and / or some additional net deposition. Although the moats apparently show some additional deposition since MY 9 (Thomas et al., 2005), and thus may show pauses in erosion, the other indicators of a roughly constant average rate of scarp recession for at least two different units, suggest longer extrapolations are useful and these possible interruptions were short.

6.3. Future lifespan of units

We have measured the minimum distances between pits or across mesas in the different units to estimate the range of time possibly required to eliminate those deposits if no new pits are initiated. Table 3 lists the results of these measures and the estimated times needed to remove the last portions of these units. All of these units could survive several Mars decades and surviving well over a Mars century is possible. With all these units already existing (undergoing erosion) for 40–130 ♂y total lifetimes are on the order of two Mars Centuries. The assumption of no recent pit formation is most easily defended for unit A1, less so for A0 (Fig. 6a). Some of the unit B deposits have so few pits that we suspect pits have formed at infrequent intervals during their exposure time. New pits are observed to form in recent Mars years in HiRISE images of unit B, but most of these are near scarps or along fractures. The amalgamated statistics of pits in unit B, Fig. 6d, do suggest that pits have continued to form in some parts of unit B, even if scarce in the limited areas selected in Fig. 6b. Some of these surfaces may well develop only a few new pits and thus could last a large fraction of the lifetimes estimated in Table 3. A future residual cap lifetime of Mars centuries was obtained by Byrne and Ingersoll (2003a) on the basis of pit size distribution and early, estimated erosion rates made before detailed multi-year rate measurements were available.

Table 3
Future lifetime estimates of some RSPC units.

Unit	Rate[a] (m/♂y)	Max dist. (m)	Typical dist. (m)	Max time (♂y)	Typical time (♂y)
A0	4.4	1580	650	179	74
A1	3.6	850	400	118	56
B	2.4	1000	420	208	86

[a] Rate is single-face retreat m/Mars year.

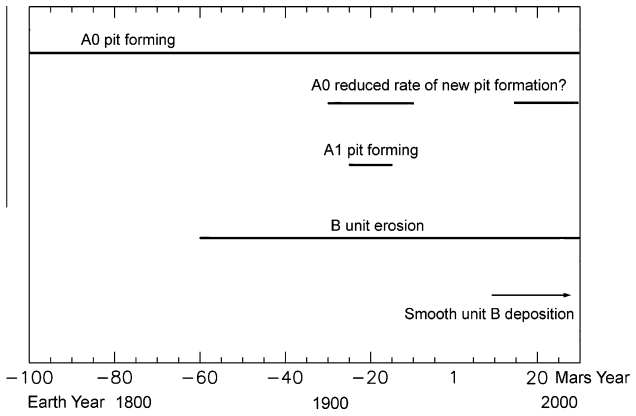

Fig. 8. Process timescales for the RSPC. Periods of different processes based on ages of pit populations in Fig. 7. The formation of pits in A0 is schematically continued to the present, but the last 10–20 Mars years may be have been a period of reduced formation from the data in Fig. 6a; note also Fig. 7. A few A1 pits have formed more recently than those at ~−MY 20 (Figs. 6 and 7), but this plot has been made generalized for clarity.

6.4. Timescale summary

An approximate accounting of the processes inferred from the above analysis is shown in Fig. 8. These results are modestly different from previous ones (Thomas et al., 2005, 2009), but with the much better constraints on erosion rates and the stronger conclusion that extrapolation backwards is warranted, there is a much firmer picture of broad changes in processes.

An apparent change in the formation of A0 pits seems to coincide with the period of initiation of A1 depressions. However, the distribution of A0 pit sizes might instead indicate a change in erosion rate: a significantly higher erosion rate that slowed around MY 1 could compress the crudely bimodal calculated ages of A0 pits into one distribution starting at a younger age. This model would then mean that A0 erosion slowed when A1 erosion effectively began. Such a higher earlier rate would have to be nearly twice the current one. Without good physical models of how the erosion proceeds, such a juxtaposition of counter intuitive events is not well supported. Under any circumstance, the existence of A0 before Mars year −100 is highly likely. Its formation time, if involving a continuing thermal imbalance of the order modeled by Bonev et al. (2002, 2008) and Thomas et al. (2009), would need ~10 ♂y per m depth, or up to 140 ♂y to accumulate the maximum thicknesses. Unit A1 could have formed in less time, perhaps 90 ♂y. The difficulty of associating A1 and A0 stratigraphically (Thomas et al., 2009) means unit A1 could be simply a contemporary, thinner facies of A0, or a later deposition in regions mostly free of A0. Certainly the geography of deposition in the RSPC has not been well examined and might yet reveal diagnostic patterns.

7. Deposition and erosional mechanisms

7.1. The upper surface: what is happening while the scarps retreat?

Detection of m/♂y scarp retreat is relatively simple with high-resolution nadir imaging. Detecting small vertical changes in near-nadir images is much more challenging. Vertical erosion has been inferred in a few sites from shadow length measurements (Bryson et al., 2008; Blackburn et al., 2010). Vertical changes have been included in models of generalized residual cap morphology (Byrne, 2011). Thermal balance calculations suggest the possibility of annual deposition or erosion of ~10 cm of CO_2 ice dependent upon expected variations in atmospheric clarity (Bonev et al., 2002; Thomas et al., 2009).

The upper surface of the RSPC displays roughness elements even in CTX (6 m/pixel) data as well as MOC (down to 1.5 m/pixel) and HiRISE (25–50 cm/pixel). Some of the more striking forms are patterns of polygonal cracks and polygonal ridges, the latter usually only visible in HiRISE data (Figs. 9a, 9b and 9c). In some areas these forms appear to repeat from year to year, suggesting there has been very little net change in the surface cover. In other areas some changes or new ridges appear to have formed in one or 2 Mars years. The exposures of thin upper layers ≪1 m thick noted by Thomas et al. (2009) have now been observed to be removed or

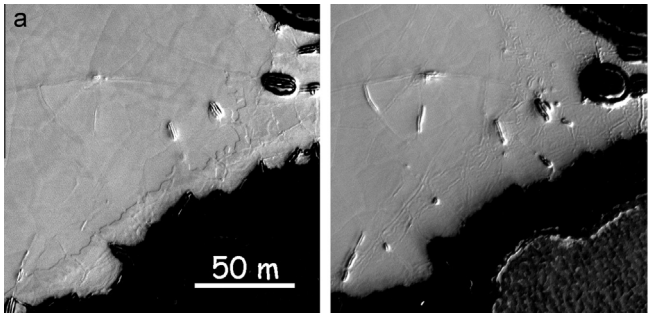

Fig. 9a. Upper surface of unit B over a 2 Mars year interval. Left: HiRISE image PSP_005701_0940, L_s = 331°, MY 28. Right: ESP_023515_0940, L_s = 338°, MY 30. Contrast highly stretched to emphasize the upper surface. Sun is from left. 85.7°S, 354.5°W.

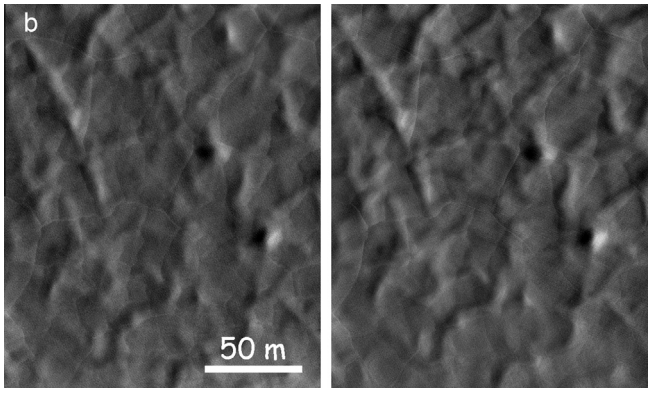

Fig. 9b. Surface of unit A0 over 2 Mars year span. Left HiRISE image PSP_005095_0930, L_s = 304°. MY 28, incidence = 69°. Right: ESP_023397_930, L_s = 333°. MY 30, incidence = 78°. Sun is from the left. Broader features are depressions, narrow forms are ridges. 86.4°S, 359.2°W.

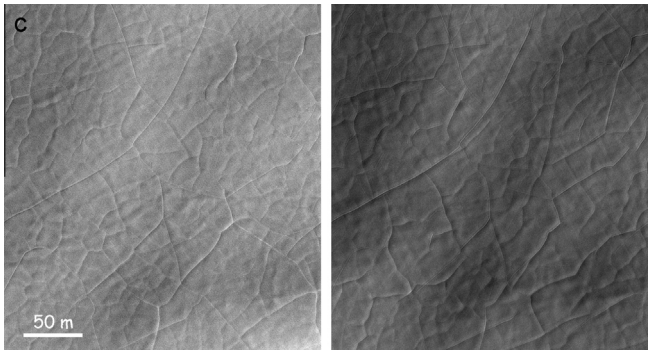

Fig. 9c. Surface of pre-Mariner 9 unit B. Left: HiRISE image PSP_005701_0940, L_s = 331°, MY 28. Right: ESP_023515_0940, L_s = 338°, MY 30. Sun is from left, most features visible are ridges. 85.7°S, 353.8°W.

covered in some instances between MY 28 and MY 30. In particular, a more thorough search of HiRISE data for the thin layers shows their exposures are usually within 25 m of scarp edges, and nearly all instances of these layers occur on unit B. These layer exposures appear to have been more prominently visible in MY 28 coverage than in subsequent years, although varying atmospheric conditions make some of the comparisons marginal. The geography of these layer exposures adds to the picture of a complicated series of events leading up to the passage of an eroding scarp past a point in the RSPC.

The seeming relative stability of the upper surfaces of A units for 2 years during periods when changes occurred nearby on the top of unit B, may partly explain the puzzle of younger unit B deposits apparently not covering unit A (Thomas et al., 2005, 2009). The concurrent changes on the upper surfaces of units A and B remain an area of future fruitful research with HiRISE data.

7.2. Other features affecting interpretations

Other features of the residual cap provide insight into changing conditions. Inverted unit A0 topography was described in Thomas et al. (2005). Basically, erosion of the thick A0 units leaves scalloped mesas of distinctive sizes and forms (radii of curvature of a few 100 m; Fig. 2a). In a few areas that are largely covered by unit B there are subtle topographic forms having the outlines of scalloped mesas, but they are topographically relatively low relative to their surroundings rather than relatively high. These forms almost certainly represent the collapse of unit A and coverage by thin amounts of unit B (Fig. 20 in Thomas et al., 2005). Collapse of unit A0 after MY 9 is observed in several places elsewhere in the RSPC (Thomas et al., 2009). The presence of inverted relief indicates a change in the relative durability of the two units, A0 somehow became much less stable than the B unit materials.

As noted in Section 5.2 there are ghosts of large A0 depressions that are largely free from A0 remnants and marked by semi- or fully circularly-symmetric patterns eroded in unit B identical to those within fully enclosed pits in unit A0. The sizes of these forms (Fig. 6a) suggest growth over a duration of ~50–60 ♂y. This erosion would have effectively been terminated at some time fairly recently given the covering by B materials and the size of superposed pits and other depressions, probably sometime after MY 1. This population of forms may have developed during the peak of A0 pit formation (shift the distribution of ghosts in Fig. 6a right about 200 m, or 20–30 ♂y) and eliminated their bounding A0 materials by scarp retreat or possibly by collapse of the sort that may be involved in the inverted relief or in the formation of "downwasted materials" (Thomas et al., 2009; Figs. 10 and 12). The possible role of collapse of unit A is suggested by the occurrence of the largest concentration of ghost forms (Fig. 4a) in the region of the best examples of inverted relief.

7.3. Constraints for models

This work is about simple interpretation of morphologic data; we have not attempted actual physical modeling of the deposition and erosion. We can, however, enumerate some of the findings that need to be matched in any effort to model the development of the RSPC in detail. Such models so far have been generalized (Byrne and Ingersoll, 2003b; Blackburn et al., 2010; Byrne, 2011) and although they include reasonable assumptions, do not yet match particular deposit morphologies or stratigraphic features.

(a) Scarp erosion rate differs between different units (Thomas et al., 2005, 2009, this work). Scarp retreat rate appears to be crudely proportional to scarp height (Thomas et al., 2009), and involves fracturing and collapse (Thomas et al., 2009; Byrne et al., 2008). It is not a simple retreat of a scarp by sublimation, though the material eventually is certainly lost by sublimation.

(b) Initiation of pit erosion in a deposit is not uniform through time (Byrne and Ingersoll, 2003a; Thomas et al., 2005, 2009, this work).

(c) The upper surface can remain virtually unchanged year-to-year in some places; in others, changes of perhaps 10 cm depth occur (Thomas et al., 2005, 2009). The upper surface of unit A appears far more stable than that of unit B (this work, especially).

(d) The only discernible layers in the RSPC deposits are $\ll$1 m in thickness (Thomas et al., 2009; this work).

(e) Collapse occurs over wide areas in unit A0 into rough debris, and compaction may occur in unit A1/A2 forming smooth deposits (Thomas et al., 2009).

8. Summary

Data through Mars year 30 show erosion of RSPC deposits by scarp retreat has occurred at approximately the same rate for at least 6 Mars years. Pit sizes and retreat rates indicate approximately current rates of erosion apply over the 21 Mars years since Mariner 9 observations. Extrapolation of current erosion rates for different units is a reasonable first approximation for estimating past erosion epochs. The thicker units appear to have undergone changes in erosion about 30–50 ♂y ago. The thinner units have some areas possibly 80 ♂y old, and younger materials over a meter thick that have accumulated since MY 9. Formation of the thicker units probably required over 100 ♂y. At present the upper surfaces of most areas, especially the thicker A units, show little change at the few-cm level over 2 Mars years. This observation suggests current conditions are substantially different from those where the thicker units were deposited. The thicker units may be reflecting variations on centuries scale; the thinner units on the few Mars decade scales.

Acknowledgments

M. Wu and L. Posiolova targeted the south polar CTX images used in this study. We thank those who targeted and made available HiRISE data so helpful to this study. A variety of help was provided by G. Benton, N. Button, B. Cantor, B. Carcich, K. Consroe, S. Davis, K. Edgett, S. Lee, M. Malin, T. Shannon. Funded in part by the Mars Reconnaissance Orbiter project. Reviews by A. Ingersoll and K. Herkenhoff notably improved this presentation.

References

Becerra, P., Byrne, S., and HiRISE Team, 2011. CO_2 Frost Halos on the South Polar Residual Cap of Mars. LPI Contributions 1323. Abstract: paper 6024, 2pp.

Blackburn, D.G., Bryson, K.L., Chevrier, V.F., Roe, L.A., White, K.F., 2010. Sublimation kinetics of CO_2 ice on Mars. Planet. Space Sci. 58, 780–791.

Bonev, B.P., James, P.B., Bjorkman, J.E., Wolff, M.J., 2002. Regression of the Mountains of Mitchel polar ice after the onset of a global dust storm on Mars. Geophys. Res. Lett. 29, 2017.

Bonev, B.P., Hansen, G.B., Glenar, D.A., James, P.B., Bjorkman, J.E., 2008. Albedo models for the residual south polar cap on Mars: Implications for the stability of the cap under near-perihelion global dust storm conditions. Planet. Space Sci. 56, 181–193.

Bryson, K., Chevrier, V., Roe, L., White, K., Blackburn, D., 2008. The Sublimation Rate of CO_2 under Simulated Mars Conditions and the Possible Climatic Implications. AAS/Division for Planetary Sciences Meeting Abstracts 40, #03.06.

Byrne, S., 2011. Simulating the landscape evolution of the martian residual CO_2 ice cap. Proc. Lunar and Planetary Institute Science Conference Abstracts 42, 2728.

Byrne, S., Ingersoll, A.P., 2003a. Martian climatic events on timescales of centuries: Evidence from feature morphology in the residual south polar ice cap. Geophys. Res. Lett. 30, 130000–130001.

Byrne, S., Ingersoll, A.P., 2003b. A sublimation model for martian south polar ice features. Science 299, 1051–1053.

Byrne, S., Russell, P.S., Fishbaugh, K.E., Hansen, C.J., Herkenhoff, K.E., McEwen, A.S., and Hirise Team, 2008. Explaining the persistence of the southern residual cap of Mars: HiRISE data and landscape evolution models. Lunar Planet. Sci. 39. Abstract 2252.

Clancy, R.T. et al., 2000. An intercomparison of ground-based millimeter, MGS TES, and Viking atmospheric temperature measurements: Seasonal and interannual variability of temperatures and dust loading in the global Mars atmosphere. J. Geophys. Res. 105, 9553–9572.

Haberle, R.M., Kahre, M.A., 2010. Detecting secular climate change on Mars. Int. J. Mars Sci. Explor. 5, 68–75.

Haberle, R.M., Kahre, M.A., Malin, M., Thomas, P.C., 2009. The Disappearing South Residual Cap on Mars: Where is the CO_2 Going? LPI Contributions 1494, pp. 19–20.

James, P.B., Kieffer, H.H., Paige, D.A., 1992. In: MarsKieffer, H.H., Jakosky, B.M., Snyder, C.W., Mathews, M.S. (Eds.), The Seasonal Cycle of Carbon Dioxide on Mars. Univ. of Arizona Press, Tucson, pp. 934–968.

James, P.B., Thomas, P.C., Malin, M.C., 2010. Variability of the south polar cap of Mars in Mars years 28 and 29. Icarus 208, 82–85.

Kahre, M.A., Haberle, R.M., 2010. Mars CO_2 cycle: Effects of airborne dust and polar cap ice emissivity. Icarus 207, 648–653.

Levinthal, E.C. et al., 1973. Mariner 9 image processing and products (K. 1). Icarus 18, 75–101.

Malin, M.C. et al., 1992. Mars observer camera. J. Geophys. Res. 97, 7699–7718.

Malin, M.C., Caplinger, M.A., Davis, S.D., 2001. Observational evidence for an active surface reservoir of solid carbon dioxide on Mars. Science 294, 2146–2148.

Malin, M.C., et al., 2007. Context camera on board the Mars reconnaissance orbiter. J. Geophys. Res. 112, E05S04. http://dx.doi.org/10.1029/2006JE002808.

McEwen, A.S., et al., 2007. Mars reconnaissance orbiter's high resolution imaging science experiment (HiRISE). J. Geophys. Res. 112, E05S02. http://dx.doi.org/10.1029/2005JE002605.

Pathare, A., Ingersoll, A., Titus, T., Byrne, S., 2005. Pitting within the martian South Polar Residual Cap: Evidence for Pressurized Subsurface Carbon Dioxide. AGU Fall Meeting Abstracts A198.

Piqueux, S., Christensen, P.R., 2008. Deposition of CO_2 and erosion of the martian south perennial cap between 1972 and 2004: Implications for current climate change. J. Geophys. Res. 113, E02006. http://dx.doi.org/10.1029/2007JE002969.

Thomas, P.C., Malin, M.C., James, P.B., Cantor, B.A., Williams, R.M.E., Gierasch, P., 2005. South polar residual cap of Mars: Features, stratigraphy, and changes. Icarus 174, 535–559.

Thomas, P.C., James, P.B., Calvin, W.M., Haberle, R., Malin, M.C., 2009. Residual south polar cap of Mars: Stratigraphy, history, and implications of recent changes. Icarus 203, 352–375.